



AUTHOR(S):

TITLE:

YEAR:

Publisher citation:

OpenAIR citation:

Publisher copyright statement:

This is the _____ version of an article originally published by _____
in _____
(ISSN _____; eISSN _____).

OpenAIR takedown statement:

Section 6 of the "Repository policy for OpenAIR @ RGU" (available from <http://www.rgu.ac.uk/staff-and-current-students/library/library-policies/repository-policies>) provides guidance on the criteria under which RGU will consider withdrawing material from OpenAIR. If you believe that this item is subject to any of these criteria, or for any other reason should not be held on OpenAIR, then please contact openair-help@rgu.ac.uk with the details of the item and the nature of your complaint.

This publication is distributed under a CC _____ license.

1 **Differential Pulse Voltammetric Determination of Albendazole and**
2 **Mebendazole in Pharmaceutical Formulations**

3 **Based on Perovskite-Type LaFeO₃ Nanoparticles Modified Sonogel Carbon**
4 **Paste Electrodes**

5 Isaac Yves Lopes de Macedo¹; Luane Ferreira Garcia¹; River Souza Magalhães²; Aparecido Ribeiro
6 de Souza²; Adélia Maria Lima da Silva³; Ieda Maria Sapateiro Torres¹; Maycon Dible Gonçalves
7 Santos³; Stephen Rathinaraj Benjamin¹; Carlos Fernandez⁴, Eric de Souza Gil^{1*}

8
9 ¹Faculdade de Farmácia, Universidade Federal de Goiás, Goiânia, GO, Brazil.

10 ²Instituto de Química, Universidade Federal de Goiás, Goiânia, GO, Brazil.

11 ³Escola de Ciências Exatas e da Computação, Pontifícia Universidade Católica de Goiás, GO,
12 Brazil

13 ⁴ School of Pharmacy and Life Sciences, Robert Gordon University, Sir Ian Wood Building,
14 Garthdee Road, AB10 7GJ, Aberdeen (UK).

15
16
17
18
19
20
21 * Corresponding author:

22 UFG - Faculty of Pharmacy

23 Av. Universitária com 1ª Avenida s/n, Setor Universitário CEP: 74605-220 - Goiânia - GO - Brazil

24 E-mail address: ericsgil@gmail.com

25 Tel.: +55 62 3209-6440; Fax: +55 62 3209-6037

26

Abstract

29 The electroanalytical sensing of albendazole and mebendazole based on Perovskite-Type
30 LaFeO₃ nanoparticles modified sonogel carbon paste electrodes has been reported for the first time.

31 The electroanalytical protocol was successfully applied for the sensing of albendazole and
32 mebendazole in pharmaceutical formulations. Benzimidazoles, such as albendazole and
33 mebendazole, are common anthelmintic agents, diffusely used throughout the world against
34 parasitic diseases.

35 Modified sonogel carbon paste electrodes with Perovskite-type LaFeO₃ nanoparticles exhibits
36 higher electrocatalytic activity and sensitivity towards the detection of albendazole and
37 mebendazole compared to the unmodified electrode.

38 The limits of detection for albendazole and mebendazole were reported to be 0.3 μM and 0.6 μM
39 respectively and the limits of quantification 0.8 μM and 1.7 μM respectively.

40 Perovskite-type LaFeO₃ nanoparticles were characterized by X-ray diffraction (XRD), fourier
41 transform infrared (FTIR), scanning electron microscopy (SEM) and transmission electron
42 microscopy (TEM).

43

44

45

46

47

48

49

50

51

52

53

54

55

56

57

58

59

60

61

62

63

64

65

66

67

68

69

Key words: Benzimidazoles, albendazole, mebendazole, LaFeO₃ nanoparticles, differential pulse voltammetry

70

71

1. Introduction

72

73 Helminthic infections are widespread in tropical countries, leading to sub growth of children,
74 lowering their cognitive and intellectual performance, decreasing the work force and thus
75 contributing to underdevelopment of nation. Therefore, besides the relevant health problems related
76 to the malnutrition and anemia, such parasitic worms impact the socioeconomic status of endemic
77 countries [1,2].

78 The control of intestinal parasites have been done mostly by the benzimidazoles, in which
79 albendazole (AB) and mebendazole (MB) are remarkable examples, that combine therapeutic
80 efficiency, broad spectrum of activity, low side effects even at large doses with low cost [1,3,4].

81 The benzimidazoles interact with β -tubulin, a eukaryotic cytoskeletal protein, thus inhibiting its
82 polymerization into microtubules and hampering the cell motility, intracellular transport of
83 cytoplasmic particles among other important biochemical functions [5]. Figure 1 depicts the
84 chemical structures of AB and MB. AB and MB also exert their mode of action by avoiding the
85 glucose captivation and by inducing some oxidative stress [1,6,].

86

Figure 1

87 Though AB presents activity against many intestinal parasites, the use to combat larval forms of
88 *Taenia solium*, that is associated to neurocysticercosis, a brain infection is one of its therapeutic
89 applications of utmost importance [7,8].

90 In turn, MB has been proved to be a very useful chemotherapeutic agent with high cure rates against
91 nematodes and being very well tolerated in mammals [3,6,9]. Hence, taking into account the
92 great consume of both anthelmintic agents, their quantitative determination in pharmaceutical
93 formulations is of great importance.

94 Literature reveals that, chromatography with UV detection has been the predominant method for
95 quantification of AB and MB in different matrices [3,7,10,11]. Nevertheless, the chromatography is
96 marked by overall high cost, which includes laborious optimization of assay conditions, frequent
97 necessity of sample pre-treatment, both leading to elevated time-consuming, and also the
98 requirement of columns, chemical standards and HPLC grade solvents, all very expensive [6,8,9].

99 On the other hand, UV spectrophotometry [12] and non-aqueous titrimetry [13] respectively, for
100 small and large amounts of these drugs are methods that eventually fail by lack of the suitable
101 accuracy, precision, sensibility and selectivity. In turn, the electroanalytical methods, are recognized
102 by their great sensitivity, modular selectivity, creativity due to no need for pre-treatment or pre-
103 separation, reduced cost for acquisition and/or maintenance of equipment and accessories and eco
104 friendly low consume of reagents [8,9,14].

105 However, despite all mentioned advantages few papers concerned to electroanalysis of AB have
106 been published [7,8,15,16] and even fewer for MB [6,9,13,17]. Among such works, the use of
107 conventional electrodes, i.e. dropping mercury [6,13], boron-doped diamond electrode [8], glassy
108 carbon (GC) rotating disk electrode [7], and just only one graphene modified electrode [9,18] keep
109 open the search for nanostructured electrodic materials.

110 Sonogel carbon electrodes (SNGCEs) are very attractive for electrochemical studies mainly due to
111 properties such as low cost, good reproducibility, good mechanical rigidity and easy manufacture
112 and modification broadening their applicability and sensitivity [19,20]. Indeed, for the fabrication of
113 efficient electrochemical sensors, several materials have been employed in order to enhance the
114 reproducibility, stability, sensitivity and selectivity. Since nanostructured metal oxides confer high
115 electron transfer kinetics and enhancement of electroactive surface area, decreasing the required
116 over potential and as consequence increasing the selectivity and sensibility, such materials are very
117 promising [21-24].

118 LaFeO_3 is a *p*-type semiconductor catalytic material of perovskite-structure (ABO_3) that hold many
119 favorable physical and chemical properties, including narrow band gap (1.2 eV), good electrical
120 conductivity and high electrochemical stability. Besides the excellent catalytic properties, LaFeO_3
121 can be used as an electrocatalyst on the fabrication of efficient electrodic materials for sensing
122 electroactive species [22,25].

123 Thus, the aim of the present study was the development of LaFeO_3 sonogel carbon paste modified
124 electrodes for the electroanalytical determination of AB and MB in pharmaceutical formulations.

125 To the best of our knowledge this is the first manuscript to report the electroanalytical sensing of
126 albendazole and mebendazole in pharmaceutical formulations utilizing modified sonogel carbon
127 paste electrodes with Perovskite-Type LaFeO_3 Nanoparticles.

128

129 **2. Materials and Methods**

130 **2.1 Materials**

131 $\text{Fe}(\text{NO}_3)_3 \cdot 9\text{H}_2\text{O}$ was purchased from Vetec Química (Brazil), starch was purchased from
132 Synth(Brazil) and methyltrimethoxysilane (MTMOS) was purchased Merck (Darmstad, Germany).
133 $\text{La}(\text{CH}_3\text{COO})_3 \cdot 1.5\text{H}_2\text{O}$ was prepared by reported procedure [25,26] and water content was
134 determined by thermogravimetric analysis (TGA). All other chemicals and solvents were of reagent
135 grade and were used without further purification. Electrolyte solutions were prepared by using high
136 analytical grade salts, which were diluted in double distilled Milli-Q water (conductivity \leq
137 $0.1 \mu\text{Scm}^{-1}$) (Millipore S. A., Molsheim, France). AB and MB of analytical grade were obtained
138 from Sigma (Saint Louis, USA). AB and MB tablets, (containing 400 mg of the active

139 pharmaceutical principle) were purchased from a local pharmacy. Stock solutions of AB and MB
140 were freshly prepared immediately prior to the experiments in ethanol. Glass capillary tubes, i.d.
141 1.15 mm, were used as the bodies for the composite electrodes.

142 **2.2 Instrumentation**

143 The TGA of the sample was performed under nitrogen ($50 \text{ cm}^3 \text{ min}^{-1}$) on a thermogravimetric (TG)
144 instruments system, model Shimadzu DTG- 60/60H. X-ray diffraction (XRD) measurements of the
145 nanosized powder LaFeO_3 were recorded in the range $10\text{-}80^\circ$ (2θ) using a Shimadzu (XRD-6000)
146 system equipped with the $\text{Cu } K\alpha$ radiation source. The XRD data were refined using the PowderX
147 software and the cell parameters were calculated using the Unitcell software applied to the peak
148 positions of all major reflections. The average diameter of the nanocrystalline domains was
149 determined from the full-width at half-maximum (fwhm) of the strongest reflection peak (112
150 reflections) using the Scherrer's equation. The scanning electron microscope (SEM) image and
151 energy dispersive X-ray Spectroscopy (EDS) were obtained on Jeol JSM 6610 microscope equipped
152 with EDS Thermo scientific NSS Spectral Imaging. Transmission electron microscope analysis
153 (TEM) were obtained on Jeol JEM 2100 equipped with EDS Thermo scientific at an acceleration
154 voltage of 200 kV by placing the powder on a copper grid to observe the morphology and size of
155 the powders.

156 Voltammetric experiments were carried out with a potentiostat/galvanostat $\mu\text{Autolab III } \text{\textcircled{R}}$
157 integrated to the GPES 4.9[®] software, Eco-Chemie, Utrecht, The Netherlands. The measurements
158 were performed in a 5.0 mL one-compartment electrochemical cell, with a three-electrode
159 system consisting of a Sonogel modified electrode, a Pt wire and the $\text{Ag/AgCl/KCl } 3\text{M}$,
160 representing the working, the counter and the reference electrodes, respectively.

161 The experimental conditions for differential pulse voltammetry (DPV) were: pulse amplitude 50
162 mV, pulse width 0.5 s and scan rate 10 mV s^{-1} . The experimental conditions for cyclic voltammetry
163 (CV) were: scan rate of 100 mV s^{-1} and scan range from 0 to 1.0 V. The DP voltammograms were
164 background-subtracted and baseline-corrected, and all voltammetric data were analyzed and treated
165 with the software Origin 6[®].

166 All experiments were done at room temperature ($21\pm 1^\circ\text{C}$) in triplicate ($n = 3$) and the main
167 electrolyte used was the phosphate buffer (PBS).

168

169 **2.3 Preparation of LaFeO_3 Nanoparticles**

170 LaFeO_3 was prepared according to a modified procedures described in previous literature [25,26].
171 Briefly, lanthanum(III) acetate hydrate (6 mM) and $\text{Fe}(\text{NO}_3)_3 \cdot 9\text{H}_2\text{O}$ (6 mM) were dissolved in 15
172 mL water and 0.5 g soluble starch was added. The turbid solution was continuously stirred at room

173 temperature and after 15 min the heating plate was raised to about 120°C. After about 5 min the
174 solution turned to a highly viscous orange gel. This (LaFeO₃)-gel was calcined in static air at 570°C
175 (heating rate 5°C /min) for 2 h yielded a nano-sized LaFeO₃ powder.

176

177 **2.4 Fabrication of Sonogel electrode modified with LaFeO₃ nanoparticles**

178 To prepare the SNGCE, the general procedure was as follows: a mixture of 500 µL of MTMOS and
179 100 µL of a 0.2 M HCl solution was insonated for 10 s. Next, 0.5 g of graphite powder was added
180 and dispersed homogeneously in the sonosol obtained. After several minutes, once the resulting
181 material had acquired enough consistency the glass capillary tubes were filled, leaving a little extra
182 mixture sticking out of the glass tube to facilitate the ulterior polishing step. After 24 h, the
183 Sonogel-Carbon electrodes were hardened and, therefore, structured. Before use, the electrodes
184 were polished with n° 1200 emery paper to remove extra composite material and wiped gently with
185 weighing paper. Electrical contact was established by inserting a copper wire into the capillary
186 tubes. Glass capillary tubes, i.d. 1.15 mm, were used as the bodies of the composite electrodes. The
187 LaFeO₃ modified SNGE was constructed by adding 3µL aliquot of this dispersion solution (1%)
188 was chosen as the modifying amount and dropped onto the surface of the bare sonogel carbon
189 electrode and dried in air at room temperature, forming the modified electrode.

190

191

192 **2.5 Preparation of standard and real samples**

193 A stock solution of AB and MB (10⁻³M) were freshly prepared and used as the stock solution by
194 dissolving it in ethanol by ultrasonic waves. These solutions were diluted up to the required
195 concentrations with the same solvent. Ten pharmaceutical tablets of AB and MB, labeled with
196 amount of 400 mg (AB) and 500 mg (MB) per tablet, were completely powdered and amount of
197 average weight of one tablet was weighted. Afterwards, a suitable amount of each sample was
198 weighed and transferred to a volumetric flask, whose remaining volume was completed with
199 deionized water to obtain the AB and MB stock solutions for each sample. These solutions were
200 subjected to sonication for 10 min and then the non-dissolved solids were filtered off. Aliquots of
201 each of the stock solutions were directly added to the supporting electrolyte solution in the
202 electrochemical cell and the respective voltammograms were recorded.

203 For the determination of albendazole in syrup (40 mg AB per 10 mL), the samples were further
204 diluted to achieve the concentration of AB in the working range. The samples were then spiked with

205 appropriate amount of AB for the experiments. The standard addition method was used for
206 analyzing the pharmaceutical samples of AB and MB for the validation of the sensor.

207

208 **3. Results and Discussion**

209 **3.1 Characterization of LaFeO₃ nanocrystals**

210 Figure 2A shows the X-ray powder diffraction pattern of the LaFeO₃ sample, which indicates the
211 formation of monophasic perovskite oxides having orthorhombic structure, the diffraction data are in
212 good agreement with JCPDS card of LaFeO₃ (JCPDS 37-1493). The average particle size of the
213 LaFeO₃ nanocrystals was about 20 nm estimated from the XRD pattern parameters according to the
214 Scherrer equation [27,29]. The FT-IR spectrum (Figure 2B) of sample displays strong absorption
215 bands about 550-400 cm⁻¹ indicating the formation of lanthanum ferrite. The 570 cm⁻¹ band is
216 attributed to the Fe–O stretching vibration. Also, can be seen weak bands in the 1300–1500 cm⁻¹
217 regions which are attributable to carbonate groups [30], despite not having been detected carbonates
218 by XRD [27].

219

Figure 2

220 The TEM images of Figure 3 indicate the presence of agglomerates of porous LaFeO₃
221 nanoparticles. The individual particles are mainly in the range of about 60 to 100 nm, but also have
222 been found particles up to about 200 nm, as previously reported in the literature [30].

223

Figure 3

224 The microstructure LaFeO₃ powder can be visualized from SEM Figure 4A and 4B. SEM images of
225 LaFeO₃ powder show that the particles' morphology are most irregular in shape. As a result some
226 particles are found to form macro-agglomerations. The particle shapes are not well defined as there
227 are many large and small pores present in the whole material with range of *ca.* 30 to 70 nm.

228

Figure 4

229 The elemental analysis of the sample was carried out by using EDS and is shown in Figure 4C. The
230 EDS result clearly shows that LaFeO₃ contains La, Fe, and O without any impurity and quantitative
231 analysis verified that doping with lanthanum is close to the expected concentration.

232

233 **3.2 Electrocatalytic response of LaFeO₃ sonogel based electrodes**

234 The optimum amount of LaFeO₃ (1 to 10 % of total paste) on the electro catalytic performance was
235 evaluated. The effect of LaFeO₃ on the electrode performance was expressive even at the small
236 proportion, thus taking into account the cost effectiveness, thus only 1% of metal oxide shown to be
237 enough.

238 Moreover the pH of the electrolyte was also investigated over the pH range from 3 to 8. It was
239 found that the highest sensitivity was observed at pH 5 (Figure 5). Therefore, further assays were
240 performed at pH 5.0.

241 The Figure 5 shows the anodic response of SNGE and LaFeO₃-SNGE electrodes against AB and
242 MB.

243 **Figure 5**

244 Figure 5 a) and b) shows the effect of the incorporation of nanosized LaFeO₃ to SNGE which leads
245 to expressive enhancement of electrocatalytic activity for both benzimidazoles.

246 Thus the LaFeO₃ modified SNGE was used for quantitative determinations of AB and MB in
247 pharmaceutical formulations.

248

249 **3.3 The effect on concentration**

250 Next, the effect of albendazole and mebendazole concentration on perovskite-type
251 LaFeO₃ nanoparticles modified sonogel carbon paste electrodes was investigated. A range of AB
252 and MB concentrations from 1 to 10.5 μM and from 2.3 to 10.0 μM respectively was explored in
253 0.1M PBS at pH 5. The investigation was carried out using DPV as it is depicted in Figure 6a and
254 6b.

255 **Figure 6**

256 Figure 6a shows the electro-oxidation of AB at height positive potential +650 mV. Figure 6b
257 illustrates the electro-oxidation of MB at height positive potential +920mV. The peak height
258 current (I_{pa}) values increases in magnitude upon the addition of AB and MB concentrations as
259 shown in Figure 6a and b. The AB and MB concentrations range from 1 to 10.5 μM and 2.3 to 10.0
260 μM respectively were plotted against the measured peak height current (I_{pa}). Figure 6a and 6b
261 displays a good linear relationship between I_{pa} and AB and MB concentrations.

262 A linear regression equation for AB was given by ($I_p/\mu A = 2.300x + 2.116$) and for MB was given
263 by ($I_p/\mu A = 2.949x + 1.3893$) with N = 8.

264 Table 1 depicts a summary of the statistical values for AB and MB such as the linear concentration
265 range (LCR); regression equation (RE); coefficient of correlation (r), limit of detection (LoD) and
266 limit of quantification (LoQ).

267 **Table 1**

268

269 The accuracy and selectivity of the electroanalytical method was further evaluated by preparing
270 standard solutions enriched with placebo. Furthermore, the repeatability (intra-assay) and
271 reproducibility (inter-day) of measurements resulted in RSD values lower than 3%, which is in
272 agreement with the actual pharmaceutical specification for regulatory issues. As a result we can
273 comment that the electroanalytical sensor showed an excellent degree of stability and robustness.

274 The assays were performed in three replicas at three different concentrations 1, 3 and
275 5 μM for AB and 2, 6 and 10 μM for MB as illustrated in Table 2.

276 **Table 2**

277 The found recovery values were very good for all concentration levels for both benzimidazoles. The
278 percentage recovery values varied from 98% to 102% which are well within the statistical values.
279 Therefore, the usual excipients employed for pharmaceutical formulation did not interfere on the
280 method accuracy.

281 **3.4 Analysis of Pharmaceutical formulations**

282 Hence, the optimized method was evaluated for pharmaceutical analysis of tablets and suspensions
283 acquired in drugstores. The samples were prepared only by dilution and filtration, with no need for
284 exhaustive sample preparation steps. The Table 3 presents the results obtained for AB and MB
285 medicines.

286 **Table 3**

287 Also, the accuracy of the proposed method was equivalent to the one obtained by the official
288 method, which were performed by local quality control laboratory accordingly to the
289 pharmacopoeia specifications.

290 The electroanalytical protocol has been successfully applied towards the detection of AB and MB in
291 pharmaceutical solutions.

292

293 **3.5 Selectivity**

294 Finally we will turn our attention to discuss selectivity, AB and MB belongs to the chemical family
295 of benzimidazoles. In this manuscript we have reported the electrochemical detection of AB and
296 MB without cross selectivity between them as they present different electro-oxidation responses AB
297 oxidizes at +650mV and MB at +920mV.

298

299 **4. Conclusions**

300 In this manuscript we have reported for the first time the successful electroanalytical sensing of AB
301 and MB using sonogel carbon paste electrodes modified with LaFeO₃ nanoparticles in an ideal
302 buffer solution as well as in pharmaceutical solutions.

303 The sensor offers a long term stability and excellent reproducibility with essentially no pre-
304 treatment or maintenance towards the routine analysis of AB and MB. A linear response is observed
305 for AB and MB over a concentrations range from 1 to 10.5 μM and 2.3 to 10.0 μM respectively in
306 0.1M PBS at pH 5. A linear regression equation for AB was given by ($I_p/\mu A = 2.300x + 2.116$) and
307 for MB was given by ($I_p/\mu A = 2.949x + 1.3893$) with N = 8.

308 The electroanalytical methodology proposed in this manuscript was successfully applied towards
309 the sensing of AB and MB in pharmaceutical solutions. Furthermore, the analyses carried out show
310 that there was no interference of the excipients present in the pharmaceutical products.

311

312 **5-Acknowledgements**

313 The authors wish to express their gratitude to CNPq (Conselho Nacional de Pesquisa) for the grant
314 Universal MCTI/CNPq N° 14/2013.

315

316 **REFERENCES**

- 317 1. C. Locatelli, R.C. Pedrosa, A.F. de Bem, T.B. Creczynski-Pasa, C.A. Cordova, D. Wilhelm-
318 Filho, A comparative study of albendazole and mebendazole-induced, time-dependent
319 oxidative stress, *Redox Rep.* 9 (2004) 89-95.
- 320 2. J. Vercruyse, J.M. Behnke, M. Albonico, S.M. Ame, C. Angebault, J.M. Bethony, D. Engels,
321 B. Guillard, T.V. Nguyen, G. Kang, D. Kattula, A.C. Kotze, J.S. McCarthy, Z. Mekonnen, A.
322 Montresor, M.V. Periago, L. Sumo, L.A. Tchuenté, T.C. Dang, A. Zeynudin, B. Levecke,
323 Assessment of the anthelmintic efficacy of albendazole in school children in seven countries
324 where soil-transmitted helminths are endemic, *PLOS Negl. Trop. Dis.* 8 (2014) e3204.
- 325 3. A.R. Gomes, V. Nagaraju, High-performance liquid chromatographic separation and
326 determination of the process related impurities of mebendazole, fenbendazole and albendazole
327 in bulk drugs, *J. Pharm. Biomed. Anal.* 26 (2001) 919-27.
- 328 4. WHO (2010), Soil-transmitted helminthiasis. Number of children treated 2007–2008:update on
329 the 2010 global target. **Wkly Epidemiol Rec** 85 (2010) 141–148, 2010.

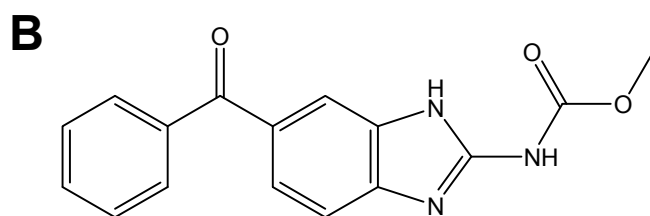
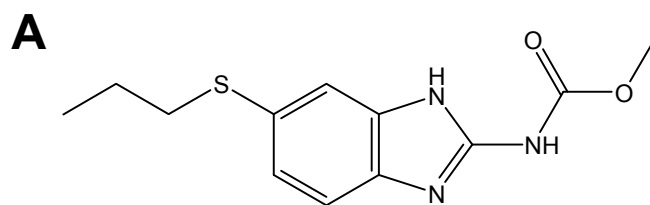
- 330 5. E. Lacey, Mode of action of benzimidazoles, *Parasitol. Today* 6 (1990): 112-5.
- 331 6. Garcia-Conesa MT, Plumb GW, Waldron KW, Ralph J, Williamson G. Ferulic acid dihydro
332 dimer from wheat bran: isolation purification and antioxidant properties of 8-O-4-diferulic
333 acid. *Redox Rep.* 3 (1997) 319–323
- 334 7. L. Santos, R. M. Takeuchi, M. P. Mariotti, M. F. De Oliveira, M. V.B. Zanoni, N. R. Stradiotto,
335 Study of electrochemical oxidation and determination of albendazole using a glassy carbon-
336 rotating disk electrode, *Il Farmaco* 60 (2005) 671–674.
- 337 8. B.C. Lourencao, M. Baccarin, R. A. Medeiros, R.C. Rocha-Filho, O. Fatibello-Filho,
338 Differential pulse voltammetric determination of albendazole in pharmaceutical tablets using a
339 cathodically pretreated boron-doped diamond electrode, *J. Electroanal. Chem.* 707 (2013) 15–
340 19.
- 341 9. M. Ghalkhani, S. Shahrokhian, Adsorptive stripping differential pulse voltammetric
342 determination of mebendazole at a graphene nanosheets and carbon nanospheres/chitosan
343 modified glassy carbon electrode, *Sensors and Actuators B: Chemical*, 185 (2013) 669- 674.
- 344 10. H. de Ruyck, R. Van Renterghem, H. de Ridder, D. de Brabander, Determination of
345 anthelmintic residues in milk by high performance liquid chromatography, *Food Control*. 11
346 (2000) 165–173.
- 347 11. K.R.A. Belaz, Q.B. Cass, R.V. Oliveira, Determination of albendazole metabolites by direct
348 injection of bovine plasma and multidimensional achiral–chiral high performance liquid
349 chromatography, *Talanta*. 76 (2008) 146–153.
- 350 12. A.C. Tella, O.M. Olabemiwo, M.O. Salawu, G.K. Obiyenwa, Developing a Spectrophotometric
351 method for the estimation of albendazole in solid and suspension forms, *Int. J. Phys. Sci.* 5
352 (2010) 379-382.
- 353 13. S. Pinzauti, E. La Porta, and G. Papeschi, DC polarography mebendazole for analysis *J. Pharm.*
354 *Biomed. Anal.*, 1 (1983) 223–228.

- 355 14. A.E. Radi, A.E El-Naggar, H.M. Nassef. Molecularly imprinted polymer based electrochemical
356 sensor for the determination of the anthelmintic drug oxfendazole, *J. Electroanal. Chem.*,
357 729(1) (2014) 135-141,.
- 358 15. A.Z. Abu Zuhri, A.I. Hussein, M. Musmar, S. Yaish, *Anal. Adsorptive stripping voltammetric*
359 *determination of albendazole at a hanging mercury drop electrode, Anal Lett.* 32 (2008) 2965–
360 2975.
- 361 16. M.F. de Oliveira, N.R. Stradiotto, *Voltammetric assay of albendazole in pharmaceutical dosage*
362 *forms, Anal. Lett.* 34 (2001) 377–387.
- 363 17. A.G.V. de Prada, M.L. Mena, A.J. Reviejo, J.M. Pingarron, *Voltammetric behavior and*
364 *determination by flow injection with amperometric detection of benzimidazoles, Anal. Lett.* 37
365 (2004) 65–79.
- 366 18. T.A.M. Msagati, J.C. Ngila, *Voltammetric determination of a benzimidazole anthelmintic*
367 *mixture at a poly(3-methylthiophene)- modified glassy carbon electrode. S. Afr. J. Chem.* 56
368 (2003) 5-9.
- 369 19. C. Ajaeroa, M.Y.M. Abdelrahimb, J.M. Palacios-Santander, M.L.A. Gil, I. Naranjo-Rodríguez,
370 J. L. Hidalgo-Hidalgo de Cisneros, L.M. Cubillana-Aguilera, *Comparative study of the*
371 *electrocatalytic activity of different types of gold nanoparticles using Sonogel-Carbon material*
372 *as supporting electrode, Sensors and Actuators B: Chemical* 172 (2012) 1244–1256.
- 373 20. A. Attar, L. M. Cubillana-Aguilera, I. Naranjo-Rodríguezc, J.L. Hidalgo-Hidalgo de Cisneros,
374 J. M. Palacios-Santander, A. Amine, *Amperometric inhibition biosensors based on horseradish*
375 *peroxidase and gold sononanoparticles immobilized onto different electrodes for cyanide*
376 *measurements, Bioelectrochemistry,*101 (2015) 84-91.
- 377 21. W. Yude, S. Xiaodan, L. Yanfena, A. Zhenlai, W. Xinghni., *Perovskite-type NiSnO₃ used as*
378 *the ethanol sensitive material, Solid State Electronic,* 44 (2000) 2009-2014
- 379 22. S. M. Khetre. *Ethanol Gas Sensing Properties of Nano-Porous LaFeO₃ThickFilm. Sensors &*
380 *Transducers,* 149 (2013) 13-19

- 381 23. W.J. Huang, S. A. De Valle, J. B. K. Kana, K. Simmons-Potter, B. G. Potter. Integration of
382 CdTe–ZnO nanocomposite thin films into photovoltaic devices 137 (2015) 6 86-92.
- 383 24. Y. Yamaguchia, Shunji Imamura, Shigeru Itoa, Keishi Nishio, Kenjiro Fujimoto, Influence of
384 oxygen gas concentration on hydrogen sensing of Pt/WO₃ thin film prepared by sol–gel
385 process. Sensors and Actuators B: Chemical, 216 (2015) 394-401.
- 386 25. D. G. Karraker, Coordination of Lanthanide Acetates, J. inorg. nucl. Chem., 31 (1969) 2815-
387 2832.
- 388 26. R. Köferstein, S.G. Ebbinghaus, Synthesis and characterization of nano-LaFeO₃ powders by a
389 soft-chemistry method and corresponding ceramics, Solid State Ionics 231 (2013) 43–48.
- 390 27. P. Ciambelli, S. Cimin, S. De Rossi, M. Faticanti, L. Lisi, G. Minelli, Ida Pettiti, P. Porta, G.
391 Russo, M. Turco, AMnO₃ (A=La, Nd, Sm) and Sm_{1-x}Sr_xMnO₃ perovskites as combustion
392 catalysts: structural, redox and catalytic properties, Appl. Catal., B Environ. 24 (2000) 243-253.
- 393 28. S.M. Khetre, H.V. Jadhav, P.N. Jagadale, S.V. Bangale, S.R. Bamane, Studies on electrical and
394 dielectric properties of LaFeO₃, Advances in Applied Science Research, 2 (2011) 503-511.
- 395 29. K. Nakamoto, Infrared and Raman Spectra of Inorganic and Coordination Compounds, 4th ed.,
396 Wiley, New York, (1986), pp. 252
- 397 30. R. Köferstein, S.G. Ebbinghaus, Synthesis and characterization of nano-LaFeO₃ powders by a
398 soft-chemistry method and corresponding ceramics, Solid State Ionics 231 (2013) 43–48.
- 399

400

401



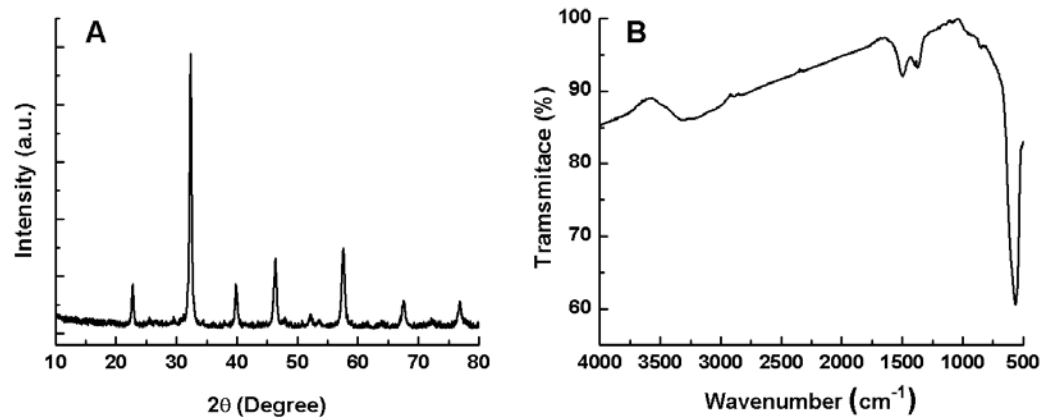
402

403

404

Figure 1. Chemical structures of albendazole (A) and mebendazole (B).

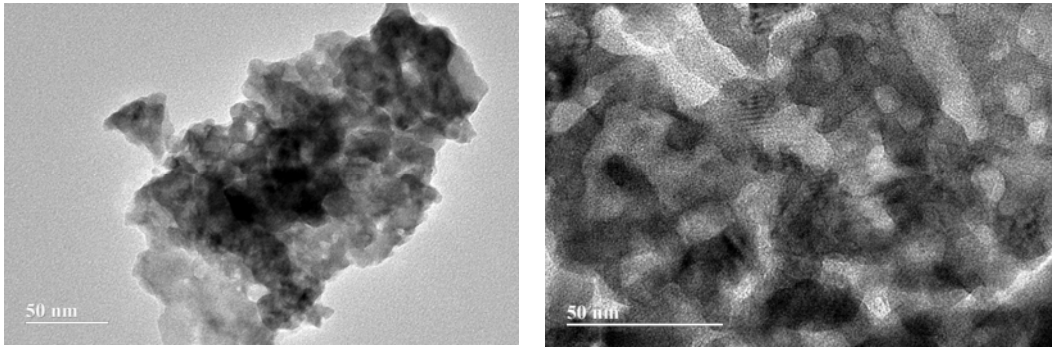
405



406

407 **Figure 2.** (A) XRD pattern of LaFeO_3 powder after being calcined at 550°C for 2h and (B) FT-IR
408 spectra of the LaFeO_3 nanoparticles.

409



410

411

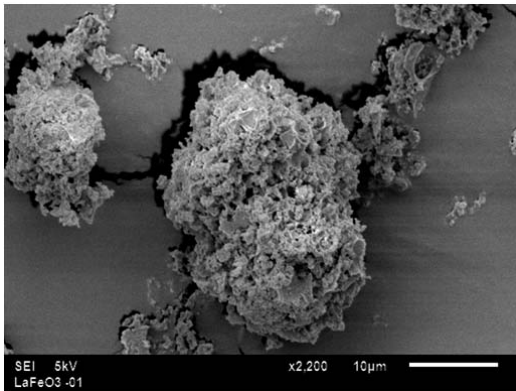
Figure 3. TEM images for LaFeO₃ nanopowders.

412

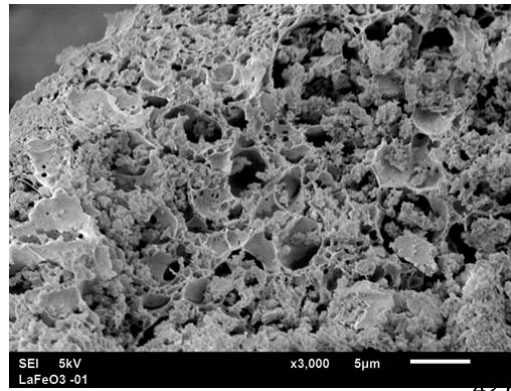
413

414

a)

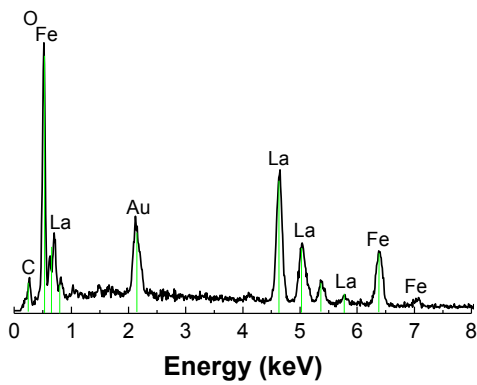


b)



415

c)



d)

Elements	% Atom
La	5%
Fe	10%
O	30%

422

423

424

425

426

427

428

429

430

431

432

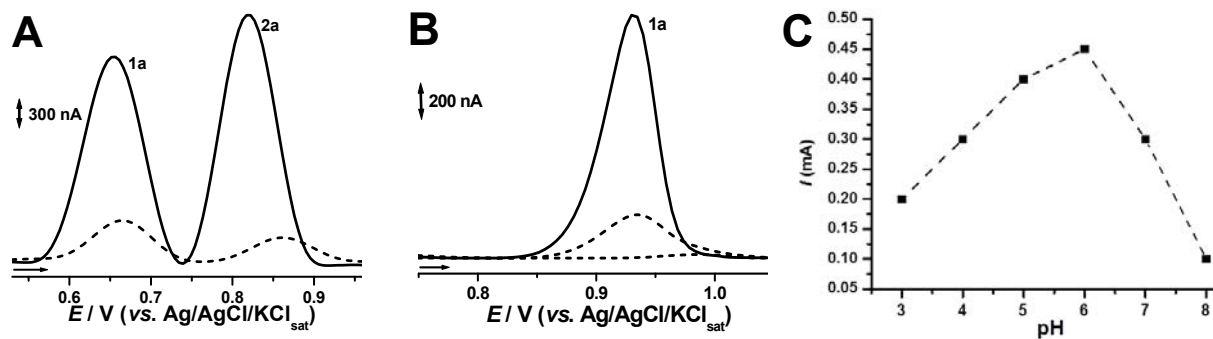
Figure 4. (a and b) SEM micrographs for LaFeO_3 nanopowders. (c) Represents the EDS spectrum with atomic percentage in table (d).

433

434

435

436



437

438

439

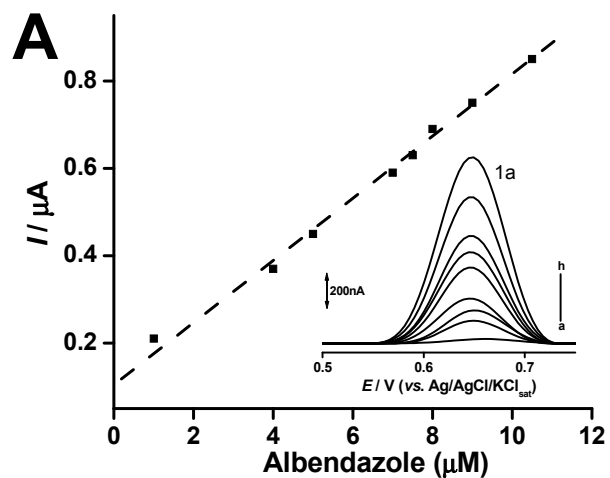
440 **Figure 5.** Differential pulse voltammograms obtained for 5 μM solutions of AB (A) and MB (B)

441 both at LaFeO₃-Sonogel (—) and at bare Sonogel (- - -) carbon paste electrode in 0.1M PBS, pH 5.0.

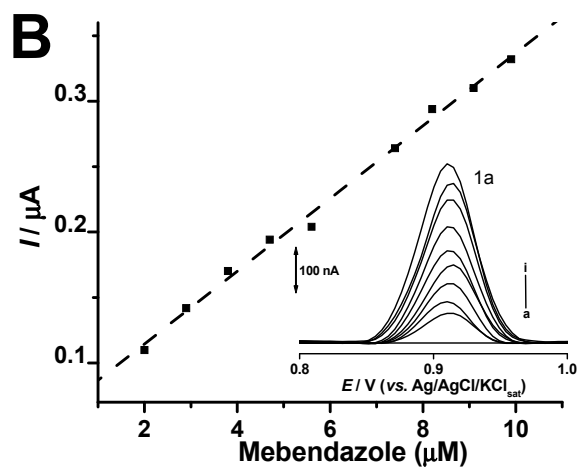
442 Relative response for 5 μM AB in different pH buffer solutions at LaFeO₃-Sonogel (C).

443

444



445



446

447

448 **Figure 6.** Calibration curves obtained for : A) AB at different concentrations a→h (1 to 10.5 μM),
449 and B) MB a→ i (2.3 to 10.0 μM) all in 0.1 M PBS, pH 5.0. Inset: the corresponding DP
450 voltammograms for increasing concentrations of AB (A) and MB (B).

451

452 **Table 1.** Statistical summary of evaluated linear concentration range (LCR); regression equation
 453 (RE); coefficient of correlation (r), limit of detection (LoD) and limit of quantification (LoQ).

Parameters	Mebendazole	Albendazole
LCR	2.3-10.0 (µM)	1.0-10.5 (µM)
LE	$Y = 2.949x + 1.3893$	$Y = 2.300x + 2.116$
r	0.9874	0.9961
intra-assay (RSD %, N = 3)	1.4	1.2
Inter-day (RSD %, N = 6)	2.7	2.5
LoD	0.6 µM	0.3 µM
LoQ	1.7 µM	0.8 µM

454 ^a SD: Standard deviation of six replicate determinations,

455 ^b RSD: relative standard deviation, Average of six replicate determination

456

457 **Table 2.** Effect of placebo on the method accuracy.

Sample	Added	Recovery	
	(μM)	Mean (μM) + SD ^a	(%)
AB	1.00	0.98 \pm 1.39	98.0
	3.00	2.97 \pm 0.89	99.6
	5.00	5.10 \pm 0.02	102.0
MB	2.00	1.98 \pm 0.16	99.0
	6.00	5.95 \pm 0.17	99.2
	10.00	9.93 \pm 0.22	99.3

458 ^aSD: Standard deviation of six replicate determinations,

459

460

461 **Table 3.** Results obtained in the determination of AB and MB in commercial pharmaceutical
462 formulations (tablets and suspensions) using the proposed DPV method.

Samples	Dosage Form	Label Concentration	Found (mg) \pm SD	Recovery (%)	Official Method Recovery (%)
AB	Tablet 1	400 mg	400.6 \pm 2.10	100.7	101.3
AB	Tablet 2	200 mg	398.3 \pm 4.44	99.50	100.1
AB	Suspension	40 mg /mL	40.0 \pm 2.22	100.6	99.1
MB	Suspension	20 mg/mL	19.5 \pm 0.53	97.5	98.0
MB	Tablet	500 mg	495.8 \pm 0.13	99.18	96.0

463 SD: Standard deviation of six replicate determinations, RSD: relative standard deviation,

464 ^aAverage of six replicate determinations

465

466 **Legends**

467 **Figure 1.** Chemical structures of albendazole (A) and mebendazole (B).

468 **Figure 2.** (A) XRD pattern of LaFeO₃ powder after being calcined at 550 °C for 2h and (B) FT-IR
469 spectra of the LaFeO₃ nanoparticles.

470 **Figure 3.** TEM images for LaFeO₃ nanopowders.

471 **Figure 4.** (a and b) SEM micrographs for LaFeO₃ nanopowders. (c) Represents the EDS spectrum
472 with atomic percentage in table (d).

473 **Figure 5.** Differential pulse voltammograms obtained for 5µM solutions of AB (A) and MB (B)
474 both at LaFeO₃-Sonogel (—) and at bare Sonogel (- - -) carbon paste electrode in 0.1M PBS, pH 5.0.
475 Relative response for 5µM AB in different pH buffer solutions at LaFeO₃-Sonogel (C).

476 **Figure 6.** Calibration curves obtained for : A) AB at different concentrations a→h (1 to 10.5 µM),
477 and B) MB a→ i (2.3 to 10.0 µM) all in 0.1 M PBS, pH 5.0. Inset: the corresponding DP
478 voltammograms for increasing concentrations of AB (A) and MB (B).

479 **Table 1.** Statistical summary of evaluated linear concentration range (LCR); regression equation
480 (RE); coefficient of correlation (r), limit of detection (LoD) and limit of quantification (LoQ).

481 **Table 2.** Effect of placebo on the method accuracy.

482 **Table 3.** Results obtained in the determination of AB and MB in commercial pharmaceutical
483 formulations (tablets and suspensions) using the proposed DPV method.